The influence of coronary plaque morphology assessed by optical coherence tomography on final microvascular function after stenting in patients with ST elevation infarction

Giovanni Luigi De Maria, MD[1,2], **Niket Patel, MBBS, BSc, MD**[1], **Mathias Wolfrum, MD**[1], **Gregor Fahrni, MD**[1], **George Kassimis, MD, MSc, PhD**[1], **Italo Porto, MD, PhD**[2], **Sam Dawkins, MBBS**[1], **Robin P. Choudhury, DM, FRCP**[3,4], **John C. Forfar, MD, PhD**[1], **Bernard D. Prendergast, DM FRCP**[1], **Keith M. Channon, MD FRCP**[1], **Rajesh K. Kharbanda, MD, PhD**[1], **Hector Manel Garcia-Garcia, MD**[5], and **Adrian P. Banning, MBBS, MD**[1]

[1]Oxford Heart Centre, NIHR Biomedical Research Centre, Oxford University Hospitals, Oxford UK

[2]Cardiovascular Department, Università Cattolica del Sacro Cuore, Rome, Italy

[3]Acute Vascular Imaging Centre, Radcliffe Department of Medicine, University of Oxford

[4]Division of Cardiovascular Medicine, BHF Centre of Research Excellence, University of Oxford

[5]MedStar Washington Hospital Center, Washington, DC, USA

Abstract

Objectives—The index of microcirculatory resistance (IMR) provides a reproducible assessment of the status of coronary microvasculature in patients with ST elevation myocardial infarction (STEMI). Frequency-domain optical coherence tomography (FD-OCT) allows detailed assessment of the morphology of coronary plaque.

We sought to determine the influence of the initial culprit coronary plaque anatomy within the infarct related artery (IRA) on IMR after stenting in STEMI.

Methods—In 25 STEMI patients IMR was measured immediately before and after stent implantation. FD-OCT imaging was performed at the same time-points and (athero)-thrombotic volume before stenting, prolapsed+floating athero-thrombotic volume after stenting, and delta (athero)-thrombotic volume were measured adopting three different strategies.

Results—There were no relationships between pre-procedural IMR and FD-OCT parameters. Pre-stenting IMR was related only to pain to wire time (p: 0.02). Irrespectively of the Method adopted, final IMR was related with pre-stenting (athero)-thrombotic volume (rho 0.44, p:0.03 for Method I, rho: 0.48, p: 0.02 for Method II and rho 0.30, p: 0.06 for Method III) and with delta (athero)-thrombotic volume (rho: 0.41, p: 0.04 for Method II and rho: 0.44, p: 0.03 for Method III).

Corresponding Author: Professor Adrian Banning, Oxford Heart Centre, Oxford University Hospitals, Headley Way, Oxford OX39DU, UK. adrian.banning@ouh.nhs.uk.

Conclusions—IMR measured before stenting is independent of the appearances of the culprit coronary plaque within the IRA. IMR after stenting, and more importantly the change in IMR after stenting, reflect the degree of distal embolization during stent implantation.

Condensed Abstract—We sought to determine the influence of the initial culprit coronary plaque anatomy within the infarct related artery (IRA) assessed by frequency-domain optical coherence tomography (FD-OCT) on coronary microvaculature function expressed by the index of microcirculatory resistance (IMR) after stenting in ST elevation myocardial infarction. A significant correlation was detected between pre-stenting IMR and ischemic time, while final IMR after stenting was directly related to pre-procedural (athero)-thrombotic volume and the change in (athero)-thrombotic volume before and after stenting. The results were consistent irrespectively of the method adopted to quantifiy the (athero)-thrombotic burden on FD-OCT.

Keywords

index of microvascular resistance; optical coherence tomography; ST elevation myocardial infarction; athero-thrombotic volume

Introduction

Primary percutaneous coronary intervention (PPCI) is the optimal treatment for ST elevation myocardial infarction (STEMI)[1]. However, even with early invasive therapy, up to 40% of patients have suboptimal myocardial perfusion despite abolition of the obstructive coronary thrombus/plaque. [2] Myocardial reperfusion indices based on coronary angiography, such as myocardial blush grade (MBG), can be used to diagnose impaired coronary flow acutely after STEMI but they cannot provide a quantitative measure. The index of microcirculatory resistance (IMR) is a readily obtained and reproducible measure of microvascular function, clinically validated against cardiac magnetic resonance imaging[3] and with a post-procedural IMR value > 40 showed to be related to worse long term clinical outcome in STEMI patients[4].

In order to improve outcomes in PPCI, a better understanding of the pathophysiology of suboptimal myocardial perfusion is necessary. Although some of the reasons for impaired final flow are likely to be unrelated to plaque characteristics (eg the door to balloon time) plaque-related factors, and especially thrombotic burden, could be relevant. Frequency-domain optical coherence tomography (FD-OCT) is a well established, high resolution (10-15 μm) intravascular imaging modality able to provide high anatomical details of the epicardial segment of coronary arteries with a level of accuracy very close to the histological analysis[5].

We aimed to undertake careful serial FD-OCT assessment of culprit plaque during STEMI and relate these appearances to IMR before and after stenting.

Methods

Patients Population

STEMI patients admitted to the Oxford Heart Centre for PPCI from January 2014 to July 2014 and recruited as part of the Ox-AMI (Oxford Acute Myocardial Infarction) study (REC number 10/H0408/24) were prospectively considered for enrolment (Figure 1). STEMI was defined as the occurrence of ongoing chest pain for at least 30 minutes associated with ST-segment elevation >2 mm in at least two contiguous leads. Exclusion criteria were symptom duration >12 h, presence of severe hemodynamic instability, severe left main disease, contraindications to adenosine infusion, plain old balloon angioplasty without stent implantation, known history of severe chronic kidney disease (estimated glomerular filtration rate < 30 ml/min), severe tortuous vessel or unfavourable anatomy for a FD-OCT study. The local ethics committee approved the protocol and the study was conducted in accordance with the Declaration of Helsinki.

PPCI was performed according to international guidelines. All patients were loaded with double antiplatelet treatment at the time of the procedure (600 mg of clopidogrel and 300 mg of aspirin in the ambulance). Anticoagulation was achieved with bivalirudin (0.75mg/kg bolus followed by an infusion of 1.75 mg/kg/min for up 4 hours after the procedure as clinically warranted). Abciximab adoption and thrombus aspiration were both left to the operator's discretion.

Angiographic and electrocardiographic analysis

Pre-stenting residual stenosis was measured by two dimensional quantitative coronary angiography (QCA) (Medcon QCA software, Medcon Limited, Tel Aviv, Israel).

Baseline pre-procedural angiographic thrombus burden was graded from 0 to 5 by thrombus score, as previously described [6]. Pre-PPCI and final TIMI flow and post-procedural MBG were assessed [7]. Angiographic distal embolization was defined as occurrence of a distal filling defect with an abrupt 'cut-off' appearance in one or more peripheral branches of the infarct related artery, distal to the PPCI site [8].

A 12-lead electrocardiogram was recorded at admission and 60 min after PPCI in all patients and ST resolution (ΔSTR) calculated as previously described, being ΔSTR defined as incomplete if less than 70% [9].

Measurement of indices of coronary phyisiology

IMR and other indices of coronary physiology (coronary flow reserve (CFR) and fractional flow reserve (FFR)) were measured, as previously described[10], soon after coronary flow restoration by thrombus aspiration and/or balloon predilation. IMR value was corrected taking into account coronary wedge pressure measured during stent balloon inflation [11].

Postdilation was left to the operator's discretion. When the operator was satisfied with the procedural result IMR, CFR and FFR were measured again and variations of all indices of coronary physiology after stenting (ΔIMR=IMR$_{\text{pre-stenting}}$−IMR$_{\text{poststenting}}$, ΔCFR=CFR$_{\text{pre-stenting}}$−CFR$_{\text{poststenting}}$, ΔFFR=FFR$_{\text{pre-stenting}}$−FFR$_{\text{poststenting}}$) were

determined. Before completion of the procedure the pressure wire was withdrawn back close to the guiding catheter to exclude pressure drift artefact.

Optical Coherence Tomography Analysis

FD-OCT analysis (Ilumien Optis System – Dragonfly Duo Imaging Catheter, St Jude Medical, Westford, MA) was performed at the same time points chosen for the measurement of IMR. Imaging was performed adopting a non-occlusive technique with automated pullback (pullback speed 36 mm/sec – 75 mm length segment imaged) during manual intracoronary injection of iso-osmolar contrast.

Off-line analysis was performed using QCU-CMS software (Medis) by two experienced operators blinded to IMR values and cases of disagreement were resolved by consensus with involvement of a third operator blinded to both IMR and previous FD-OCT data. To assess intra-observer variability, one operator repeated the measurement after 1 week on the first 20 runs (10 pre-stenting and 10 post-stenting). The same first 20 runs were analysed simultaneously by the two operators for inter-observer variability.

Definition of region of interest—As first step, the pre and post-stenting runs were exactly matched using anatomical landmarks (side branches, calcific nodules) as references for each patient. A common longitudinal region of interest (ROI) was thus identified in both pre and post-stenting runs. In the post-stenting run, ROI was defined by the stented segment. Proximal and distal edges of the stent were defined by identification of the first and last cross section of the stented segment containing stent struts in all four quadrants. The distance of these two cross sections from the previously identified anatomical landmarks was measured and used to identify the matched ROI in the pre-stenting segment (Supplementary Figure 1). Proximal and distal references were defined in both the pre- and the post-stenting runs as the segments not containing major side branches extending for a minimum of 1 mm and a maximum of 5 mm proximally and distally to the edges of the ROI, respectively. As confirmation of an accurate matching, ROI and references (both proximal and distal) had to be equal in length (same number of frames) in the pre- and post-stenting runs.

Frame by frame analysis was performed in the whole ROI (both pre- and post-stenting) while analysis was performed every 5 frames in the proximal and distal references (both pre- and post-stenting).

Pre-stenting FD-OCT measures—After checking and adjusting Z offset, contours of measured flow area ($FA_{measured}$) were first traced in each cross section, with $FA_{measured}$ corresponding to the actual lumen area (LA), in the absence of thrombus (free floating or adherent to the vessel wall) and plaque ulcerations.

Mean reference LA was calculated as the average of mean proximal and mean distal reference lumen areas (Figure 2, Panel A-B).

Athero-thombotic material was defined as a mass attached to the luminal surface or free floating within the lumen)[5]. Thrombus was classified as red if highly backscattering with

high posterior attenuation. A site of plaque rupture was identified by the presence of a cavity defined as an area cleared by contrast dye in direct communication with the lumen, located within the plaque/vessel wall and with clear identification of a "neck" or "narrow transition" [5].

Contours around floating atherothrombus area (FATA), cavity area (CA) and bridging lumen area (BLA) were then traced, with bridging lumen defined as an area cleared by contrast dye located within the thrombus and not in direct communication with the vessel wall. Within the ROI, flow area (FA) was calculated for each cross section as

FA = FAmeasured − FATA + CA + BLA (Figure 2, Panel A-C. Supplementary Figure 2)

Dissection flaps were identified and dissection length was measured as the distance from the tip of the flap to its base at the corner between the flap itself and the vessel wall[12]. Longitudinal dissection extension was calculated as the number of contiguous cross sections containing a dissection flap multiplied by 0.2 [corresponding to the thickness of a cross section (in mm) for the pre-specified pullback speed].

Thrombus burden was first assessed semiquantitatively within the ROI by measuring the arch subtending thrombus in each cross section and by calculating the COCTAIL score, as previously described [13].

Since currently there is little consensus about (athero)-thrombotic volume quantification before stenting, we measured pre-stenting (athero)-thrombotic volume according to three different methods (Figure 3).

Method I: As previously described by Kajander et al [14], thrombus area (TA) was measured in each cross section as LA minus FA. In frames with high thrombus content and consequent complex luminal border detection in more than one quadrant, LA was extrapolated from the nearest proximal or distal frame with visible lumen contour. Thrombus volume (TV) was then calculated in the whole ROI as:

$$TV = mean\ TA \times stent\ length$$

Method II: In order to guarantee the highest as possible inter-observer reproducibility no contours were traced/extrapolated behind thrombotic material attached to the vessel wall and the vessel was thus approximated to an "ideal" trunk of cone having proximal mean and distal mean reference lumen areas as baselines. Within the ROI, lumen volume, flow volume were calculated as follows

$$Lumen\ Volume = \frac{\pi}{3}L \times (R^2 + Rr + r^2)$$

$$Flow\ Volume = \sum_{i=1}^{n}(Flow\ Area_i \times h)$$

L corresponded to ROI length, R to proximal reference mean radius, r to distal reference mean radius and h to cross section thickness known to be 0.2 at the pre-specified pullback speed.

Because of the initial approximation, this method in theory cannot distinguish thrombus burden from athero-thrombus burden and thus athero-thrombus volume (ATV) was measured as follows

$$ATV = \text{Lumen Volume} - \text{Flow Volume}$$

Method III: Similar to Method II no contours were traced behind thrombotic material and the vessel was this time approximated to an "ideal" cylinder having mean reference lumen area as a baseline.

Athero-thrombus area (ATA) and ATV were calculated as follows

$$ATA = \text{mean reference LA} - FA$$

$$ATV = \sum_{i=1}^{n} (ATA_i \times h)$$

with h corresponding again to a cross section thickness of 0.2 at the pre-specified pullback speed.

In this method, ATA was assumed to be zero in cross sections with positive remodelling (eg with FA > mean reference LA).

Post-stenting FD-OCT measures—In the post-stenting run, stent struts were first identified and then labelled as uncovered vs. covered or apposed vs. malapposed. A strut was defined as covered in the presence of tissue/thrombus sitting on its luminal surface or at its both sides, and malapposed if the distance between its luminal surface and the vessel wall was greater than the strut+polymer thickness (variable according to stent size and manufacture)[5]. Percentages of covered, uncovered and malapposed struts were calculated.

After stent struts identification, LA and stent area (SA) contours were traced along with FATA and BLA contours if present. Dissection flaps were identified and measured as in the pre-stenting run.

Prolapsed athero-thrombus thickness and prolapsed athero-thrombus area (PATA) as well as stent malapposed thickness and stent malapposed area (MA) were automatically measured by the software. Prolapsed and floating athero-thrombotic area (PFATA), prolapsed and floating athero-thrombus volume (PFATV) and malapposed volume (MV) were calculated as follows[15, 16] (Figure 4)

$$PFATA = PATA + FTA - BLA$$

$$PFATV = \sum_{i=1}^{n}(PFATA_i \times h)$$

$$MV = \sum_{i=1}^{n}(MA_i \times h)$$

Delta atherothrombotic volume (ATV = Total ATV – Total PFATV) was in the end calculated. Notably ATV was calculated using ATV quantified according to methods II and III only. No ATV was calculated for Method I since this approach is supposed to take into account only thrombus and not atherosclerotic plaque, which is conversely included in total PFATV.

Statistical Analysis

All variables were expressed as mean and (±) standard deviation or as median accompanied by interquartile range, as appropriate. Normal distribution of continuous variables was verified by Shapiro-Wilk test. Frequencies were expressed as number (percentage) and compared by application of Chi Square test or Fisher exact test.

Comparisons between continuous variables under investigations were performed by Mann Whitney, and Kruskall Wallis tests, as appropriate, since not normally distributed. Correlations were tested by application of rho Spearman coefficient. Statistical analysis was performed using SPSS 22.0 (SPSS, Inc Chicago, Illinois) and p values <0.05 were considered statistically significant.

Results

Clinical and procedural characteristics

25 STEMI patients recruited within the OxAMI study having both pre- and post-stenting FD-OCT and IMR measurements were included in the current analysis. Clinical and procedural characteristics of patients are summarized in Table 1. Most patients were male (88.8%) and treated within 6 hours of symptom onset (84%), and only a small proportion of patients had established diagnosis of diabetes mellitus (8%). Notably, no patients with a very large angiographic thrombotic burden (thrombus score = 5) were observed within this selected cohort. Thrombus aspiration (92%), second generation drug eluting stents (88%) and postdilation (80%) were adopted in the vast majority and the occurrence of MBG< 2 and or incomplete STR was detected in 24% of these patients.

Indices of coronary physiology

FFR, CFR and IMR before and after stenting in the enrolled cohort are reported in Supplementary Table 1. Stenting resulted in a significant improvement in all indices of coronary physiology (FFR from 0.73 (0.63 – 0.80) to 0.93 (0.90 – 0.98), p< 0.001; CFR

from 1.15 (1.00 – 1.24) to 1.27 (1.10 – 1.83), p: 0.01; IMR from 46.4 (32.3 – 73.3) to 27.45 (15.16 – 43.74), p: 0.001) (Supplementary Table 1).

Frequency-domain optical coherence tomography derived parameters

Pre- and post-stenting FD-OCT derived parameters are summarized in Table 2. Inter- and intra-observer reproducibility for mean LA and SA measurements were 0.95 and 0.96, and 0.98 and 0.97, respectively (both p< 0.001).

Inter- and intra-observer reproducibility for TV quantification was 0.85 (p: 0.02) and 0.90 (p< 0.001) respectively for Method I and reproducibility for ATV quantification was 0.95 (p< 0.001) and 0.98 (p < 0.001) respectively for both Method II and III. In Method III, the number of cross-sections with a zeroed value of ATV was 15 (6 -27), accounting for a percentage of cross-sections with zeroed ATV per patient of 12% (5 – 24).

TV detected by Method I resulted correlated to ATV measured by Method II and III (rho: 0.50, p: 0.01 and rho: 0.46, p: 0.02, respectively). Conversely a better correlation was observed between ATV measured by Method II and III (rho: 0.97, p< 0.001).

No dissection flaps were detected in any pre-stenting run and 48% of patients presented clear FD-OCT hallmarks of plaque rupture. Red thrombus was detected in 36% of patients and COCTAIL score was 96.0 (80.5 – 179.5).

TV was 14.65 mm^3 (7.13 – 35.98) according to Method I, and ATV 67.59 mm^3 (43.90 – 96.40) according to Method II and 68.01 mm^3 (44.76 – 111.40) according to Method III.

In the post-stenting run, 32% of patients presented a dissection flap which was intrastent in all cases and with a longitudinal extension of 0.07 mm (0.04 – 1.35). 52.42% (37.32 – 64.89) of stent struts resulted to be covered and 2.90% (0.43 – 7.09) acutely malapposed. Post-stenting PFATV resulted to be 10.79 mm^3 (7.60 – 17.47).

Relationship between indices of coronary physiology and FD-OCT derived measures

The main correlations between indices of coronary physiology and FD-OCT derived parameters are summarized in Supplementary Table 2. Except for the expected inverse relationship between pre-stenting minimal LA and pre-stenting minimal lumen diameter with pre-stenting FFR and CFR (rho 0.72, p< 0.001 and rho: 0.43, p: 0.03, respectively) no further significant correlations were observed at both pre- and post-stenting time points.

Similarly no significant relationship was observed between pre- and post-stenting indices of coronary physiology and the presence of red thrombus or plaque rupture (Supplementary Figures 3 and 4).

Notably, pre-stenting IMR correlated with pain to wire time (3 hours, 27.29 [18.10 – 44.24]; 3-6 hours 53.76 [30.55 – 66.25];   6 hours, 83.42 [75.97 – 149.83]; p<0.02).

Post-stenting IMR was related with pre-stenting TV obtained from Method I(rho 0.44, p: 0.03) and with pre-stenting ATV derived from Method I and II (rho: 0.48, p: 0.02 and rho 0.30, p: 0.06, respectively) and with   ATV (rho: 0.41, p: 0.04 for Method II and rho: 0.44, p:

0.03 for Method III) (Figure 5). Notably a significant inverse correlation was present between IMR and ATV (rho: -0.53, p: 0.007 for Method II; rho -0.54, p: 0.005 for Method III)(Figure 5 and Table 3).

Discussion

In this study, FD-OCT has been used to assess culprit plaque in patients presenting with myocardial infarction. These appearances before and after stenting were compared with the changes in indices of coronary physiology during revascularisation. There was a close relationship between pre-procedural minimal LA and minimal lumen diameter and FFR and CFR prior to stent deployment. The change in TV and ATV was closely related to the change in IMR at completion of PPCI. However, no relationship was observed between pre-procedural IMR and epicardial stenosis degree, atherothrombotic burden and hallmarks of plaque instability (plaque rupture or red thrombus).

IMR has recently been shown to have good accuracy in detecting the degree of microvascular impairment in STEMI patients [4] and it could be measured soon after flow restoration becoming a potential risk-stratification tool in the very early stage of PPCI [10, 17].

In the current study, we have used FD-OCT to investigate the anatomical factors influencing IMR and its evolution after PPCI in STEMI patients for the first time. The first observation that pre-procedural IMR is not related to any FD-OCT parameter highlights the fact that none of the features of the culprit plaque influence the value of pre-stenting IMR. This independence of pre-stenting IMR from epicardial anatomical features is consistent with previous observations showing the lack of relationship between IMR and the degree of epicardial stenosis degree in the setting of stable CAD[11, 18]. Moreover, this observation is further corroborated by the relationship between pain to wire time and pre-stenting IMR, suggesting that the magnitude of the ischemic insult is the dominant factor in determining the degree of initial coronary microvasculature impairment [10]. Interestingly no relationship was observed between IMR (both pre- and post-stenting) and the presence of plaque rupture, providing additional pathophysiological insight into the outcomes of the OCTAVIA study which failed to detect a difference in clinical outcomes at two years in STEMI patients with and without signs of ruptured plaque[19].

Previous studies have suggested a relationship between the presence of red thrombus retrieved during thrombus aspiration[20] and the likelihood of microvascular impairment. In this study, red thrombus was observed in only 36%. This may explain why we could not detect any correlation between red thrombus and microvascular impairment in this cohort and covert selection bias may account for this.

Pre-procedural FD-OCT defined athero-thrombotic burden presented a relationship with post-procedural IMR confirming the previous finding that angiographic thrombus score predicts the final IMR value[10]. This is further extended by the correlation of final IMR and IMR with ATV. Even though it is not possible to exclude that a certain percentage of thrombus may remain trapped behind the stent struts, it is plausible that ATV is actually a

measure of the amount of embolized material, supporting the strict relationship between distal embolization and IMR. These results are in keeping with previous studies in the setting of stable CAD showing a relationship between delta atherosclerotic burden and troponin rise [21] as well as a greater occurrence of microvascular impairment in patients with thin fibrous cap atherosclerotic plaque, known to be at higher risk of distal embolization[22].

In this study, ATV before stenting was quantified according to three different methods, as a reflection of the actual uncertainty about the best way to measure pre-stenting atherothrombotic burden with FD-OCT. Beside the already published methodology (Method I) proposed by Kajander et al[14], we presented two other methods for the quantification of ATV. Compared to Method I, both Method II and III present good reproducibility, are easier to perform relying only on flow area measurement, without the need for extrapolating contours behind thrombus. Additionally, both methods take into account thrombotic and atherosclerotic burden at the same time, as indicated by the higher values of ATV if compared with Method I. However it must be acknowledged that because of the approximation of the vessel to an ideal trunk of cone or to a cylinder these two methods have the risk of ignoring both positive or extreme negative vessel remodelling with possible underestimation and overestimation of the true thrombotic burden, respectively. The comparison of the three quantification strategies is beyond the aim of this study, even though we recognize that a future study to identify the optimal method with the best accuracy and reproducibility may be warranted. However, the observation that the correlation between IMR and athero-thrombotic burden was maintained, irrespectively of the method adopted, gives validity to our findings.

In conclusion, this study adds useful elements to our understanding of the evolution of the coronary microvasculature in response to stenting in STEMI. Understanding these aspects may be relevant when IMR is proposed as a potential future diagnostic and decision making tool for the management of STEMI patients undergoing PPCI.

Limitations

The small sample size is a limiting factor within this study but the complexity of the collected data makes this cohort unique. FD-OCT analysis was focused on the definition of atherothrombotic burden with no details provided concerning other atherosclerotic plaque features, such as fibrous cap thickness, lipid core and calcium content. However, given the observed results, it is quite unlikely that any of these variables would have been significantly related with indices of coronary physiology. Moreover, it must be recognized that the high content of thrombus related to the specific clinical presentation of the patients recruited would have made this kind of analysis difficult and only possible outside the culprit site segment. Similarly it has to be noted that in the presence of red thrombus, lumen border detection becomes unclear because of high backscattering making athero-thrombus burden measurement complex. In the current manuscript we overcame this by using three different methods to assess ATV. Notably, methods II and III are unaffected by red thrombus high backscattering. Ideally a combination of FD-OCT with intravascular ultrasound could also

have directly addressed this limitation, at the cost of increased study protocol complexity in an unstable clinical setting.

It should be noted that FD-OCT was performed immediately before stenting and thus after lesion preparation with manual thrombectomy and/or predilation. This is a modification of the initial ATV burden and what has been measured is the actual residual athero-thrombotic burden. However, this limitation does not affect the purpose of the study aiming to assess the relationship between coronary microvasculature status and culprit lesion morphology before and after stenting.

Supplementary Material

Refer to Web version on PubMed Central for supplementary material.

Acknowledgements

Abbreviations

ATA	atherothrombotic area
ATV	atherothrombotic volume
BLA	bridging lumen area
CA	cavity area
CAD	coronary artery disease
CFR	coronary flow reserve
FATA	floating athero-thrombotic area
FD-OCT	frequency domain optical coherence tomography
FFR	fractional flow reserve
IMR	index of microcirculatory resistance
IRA	infarct related artery
LA	lumen area
MA	malapposed area
MV	malapposed volume
PFATV	prolapsed+floating athero-thrombotic volume
PPCI	primary percutaneous coronary intervention

ROI	region of interest
SA	stent area
STEMI	ST elevation myocardial infarction
TA	thrombus area
TV	thrombus volume
ATV	delta athero-thrombotic volume
IMR	delta IMR

References

1. Windecker S, Kolh P, Alfonso F, Collet JP, Cremer J, Falk V, et al. 2014 ESC/EACTS Guidelines on myocardial revascularization. Eur Heart J. 2014 Oct 1.35:2541–619. [PubMed: 25173339]

2. Morishima I, Sone T, Okumura K, Tsuboi H, Kondo J, Mukawa H, et al. Angiographic no-reflow phenomenon as a predictor of adverse long-term outcome in patients treated with percutaneous transluminal coronary angioplasty for first acute myocardial infarction. J Am Coll Cardiol. 2000 Oct.36:1202–9. [PubMed: 11028471]

3. McGeoch R, Watkins S, Berry C, Steedman T, Davie A, Byrne J, et al. The index of microcirculatory resistance measured acutely predicts the extent and severity of myocardial infarction in patients with ST-segment elevation myocardial infarction. JACC Cardiovasc Interv. 2010 Jul.3:715–22. [PubMed: 20650433]

4. Fearon WF, Low AF, Yong AS, McGeoch R, Berry C, Shah MG, et al. Prognostic value of the Index of Microcirculatory Resistance measured after primary percutaneous coronary intervention. Circulation. 2013 Jun 18.127:2436–41. [PubMed: 23681066]

5. International Working Group for Intravascular Optical Coherence Tomography (IWG-IVOCT). Consensus standards for acquisition, measurement, and reporting of intravascular optical coherence tomography studies: a report from the International Working Group for Intravascular Optical Coherence Tomography Standardization and Validation. J Am Coll Cardiol. 2012; 59:1058–72. [PubMed: 22421299]

6. Sianos G, Papafaklis MI, Serruys PW. Angiographic thrombus burden classification in patients with ST-segment elevation myocardial infarction treated with percutaneous coronary intervention. J Invasive Cardiol. 2010; 22:6B–14B. [PubMed: 20048390]

7. van 't Hof AW, Liem A, Suryapranata H, Hoorntje JC, de Boer MJ, Zijlstra F. Angiographic assessment of myocardial reperfusion in patients treated with primary angioplasty for acute myocardial infarction: myocardial blush grade. Zwolle Myocardial Infarction Study Group. Circulation. 1998; 97:2302–6. [PubMed: 9639373]

8. Napodano M, Ramondo A, Tarantini G, Peluso D, Compagno S, Fraccaro C, et al. Predictors and time-related impact of distal embolization during primary angioplasty. Eur Heart J. 2009; 30:305–13. [PubMed: 19153179]

9. Sorajja P, Gersh BJ, Costantini C, McLaughlin MG, Zimetbaum P, Cox DA, et al. Combined prognostic utility of ST-segment recovery and myocardial blush after primary percutaneous coronary intervention in acute myocardial infarction. Eur Heart J. 2005; 26:667–74. [PubMed: 15734768]

10. De Maria GL, Cuculi F, Patel N, Dawkins S, Fahrni G, Kassimis G, et al. How does coronary stent implantation impact on the status of the microcirculation during primary percutaneous coronary intervention in patients with ST-elevation myocardial infarction? Eur Heart J. 2015 Aug 7.36:3165–77. [PubMed: 26254178]

11. Layland J, MacIsaac AI, Burns AT, Somaratne JB, Leitl G, Whitbourn RJ, et al. When collateral supply is accounted for epicardial stenosis does not increase microvascular resistance. Circ Cardiovasc Interv. 2012; 5:97–102. [PubMed: 22319068]

12. Radu MD, Räber L, Heo J, Gogas BD, Jørgensen E, Kelbæk H, et al. Natural history of optical coherence tomography-detected non-flow-limiting edge dissections following drug-eluting stent implantation. EuroIntervention. 2014; 9:1085–94. [PubMed: 24064426]

13. Prati F, Capodanno D, Pawlowski T, Ramazzotti V, Albertucci M, La Manna A, et al. Local delivery versus intracoronary infusion of abciximab in patients with acute coronary syndromes. JACC Cardiovasc Interv. 2010; 3:928–34. [PubMed: 20850091]

14. Kajander OA, Koistinen LS, Eskola M, Huhtala H, Bhindi R, Niemelä K, et al. Feasibility and repeatability of optical coherence tomography measurements of pre-stent thrombus burden in patients with STEMI treated with primary PCI. Eur Heart J Cardiovasc Imaging. 2015; 16:96–107. [PubMed: 25240168]

15. Muramatsu T, García-García HM, Lee IS, Bruining N, Onuma Y, Serruys PW. Quantitative optical frequency domain imaging assessment of in-stent structures in patients with ST-segment elevation myocardial infarction: impact of imaging sampling rate. Circ J. 2012; 76:2822–31. [PubMed: 22971949]

16. Onuma Y, Thuesen L, van Geuns RJ, van der Ent M, Desch S, Fajadet J, et al. Randomized study to assess the effect of thrombus aspiration on flow area in patients with ST-elevation myocardial infarction: an optical frequency domain imaging study--TROFI trial. Eur Heart J. 2013; 34:1050–60. [PubMed: 23396493]

17. De Maria GL, Fahrni G, Alkhalil M, Cuculi F, Dawkins S, Wolfrum M, et al. Procedural prediction of outcome of reperfusion in ST elevation myocardial infarction using Age, Thrombotic burden and index of microcirculatory resistance (ATI score). EuroIntervention. 2016 Accepted for publication.

18. Yong AS, Ho M, Shah MG, Ng MK, Fearon WF. Coronary microcirculatory resistance is independent of epicardial stenosis. Circ Cardiovasc Interv. 2012; 5:103–8. [PubMed: 22298800]

19. Saia F, Komukai K, Capodanno D, Sirbu V, Musumeci G, Boccuzzi G, et al. Eroded Versus Ruptured Plaques at the Culprit Site of STEMI: In Vivo Pathophysiological Features and Response to Primary PCI. JACC Cardiovasc Imaging. 2015; 8:566–75. [PubMed: 25890582]

20. Yunoki K, Naruko T, Sugioka K, Inaba M, Iwasa Y, Komatsu R, et al. Erythrocyte-rich thrombus aspirated from patients with ST-elevation myocardial infarction: association with oxidative stress and its impact on myocardial reperfusion. Eur Heart J. 2012; 33:1480–90. [PubMed: 22240493]

21. Porto I, Selvanayagam JB, Van Gaal WJ, Prati F, Cheng A, Channon K, et al. Plaque volume and occurrence and location of periprocedural myocardial necrosis after percutaneous coronary intervention: insights from delayed-enhancement magnetic resonance imaging, thrombolysis in myocardial infarction myocardial perfusion grade analysis, and intravascular ultrasound. Circulation. 2006; 114:662–9. [PubMed: 16894040]

22. Yamada R, Okura H, Kume T, Neishi Y, Kawamoto T, Miyamoto Y, et al. Target lesion thin-cap fibroatheroma defined by virtual histology intravascular ultrasound affects microvascular injury during percutaneous coronary intervention in patients with angina pectoris. Circ J. 2010; 74:1658–62. [PubMed: 20595776]
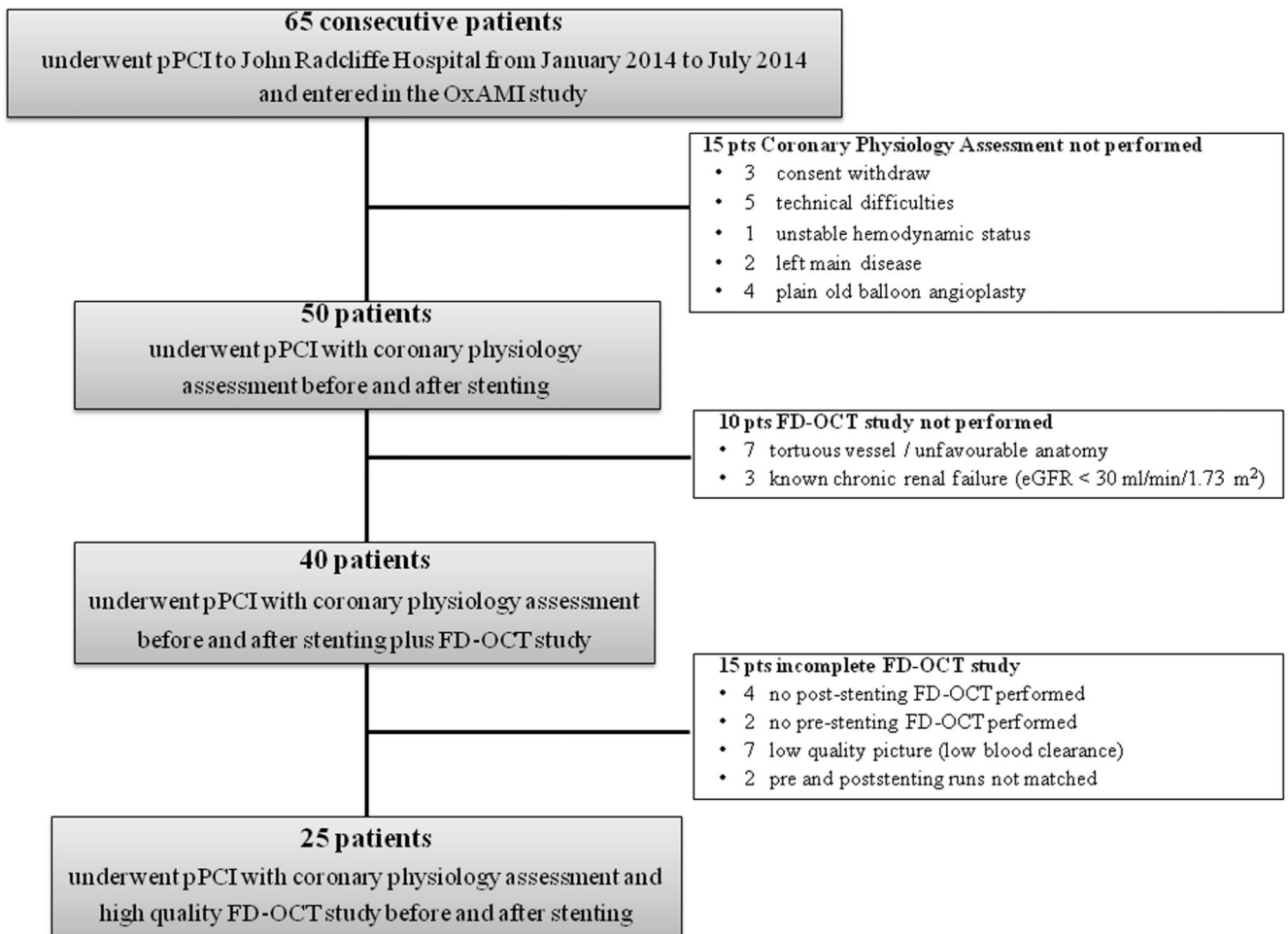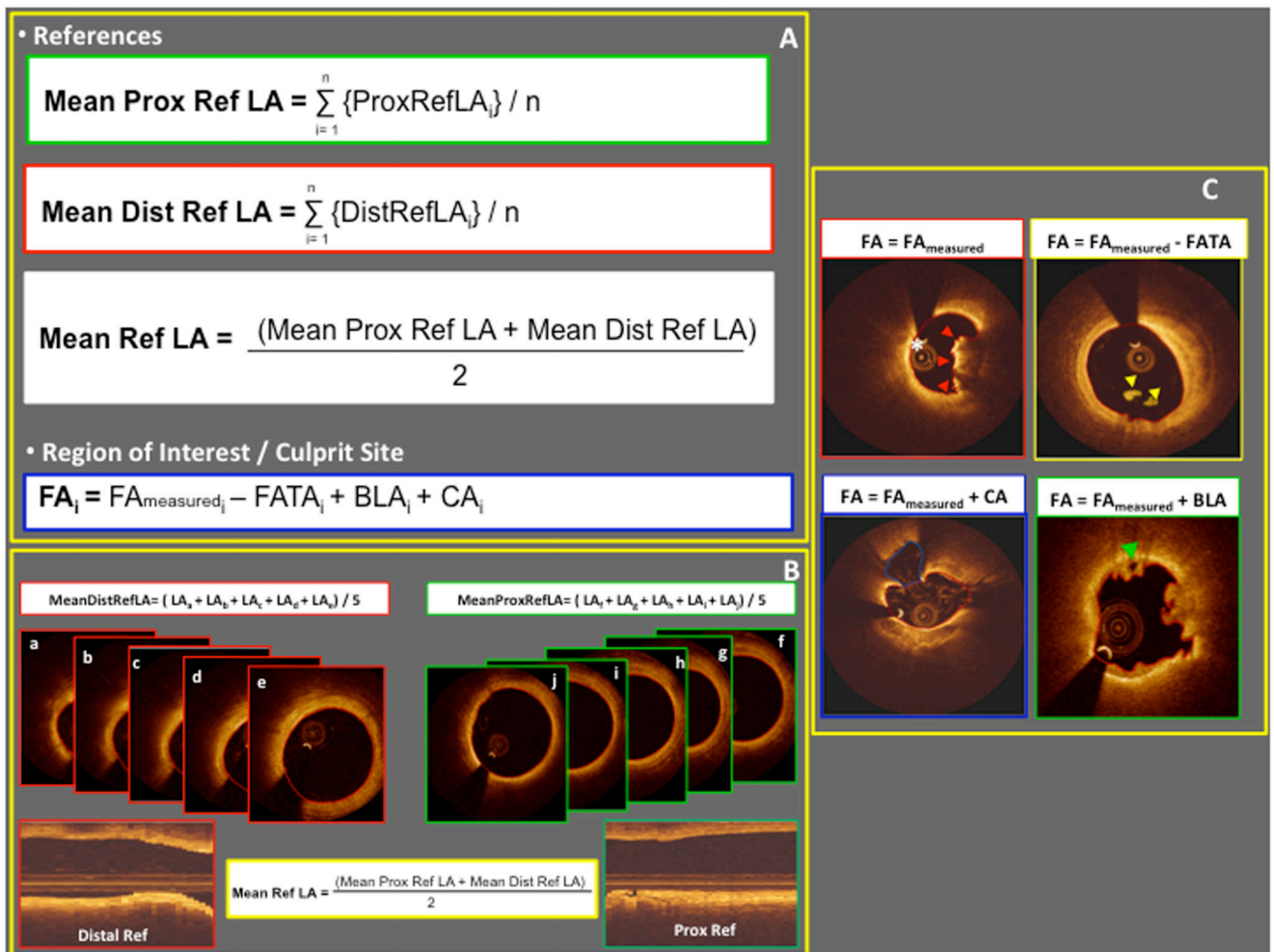
Figure 1. Study Flow Chart.

Figure 2. Pre-stenting FD-OCT run measures.
Panel A and B. Mathematical formulae adopted to calculate mean reference lumen areas and flow areas. Panel C. Calculation of flow area according to the presence of thrombus adherent to the vessel wall (red arrowheads), floating thrombus (yellow arrowheads), cavity associated with plaque rupture (white asterisk), and bridging lumen within the thrombus (green arrowhead). Note that contours of meausured flow area are highlighted in red in each image of Panel C. (BLA: bridging lumen area; CA: cavity area; FA: flow area; $FA_{measured}$: measured flow area; FATA: floating atherothrombus area; LA: lumen area; ref: reference; ROI: region of interest)
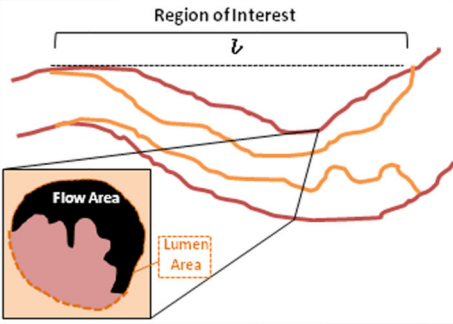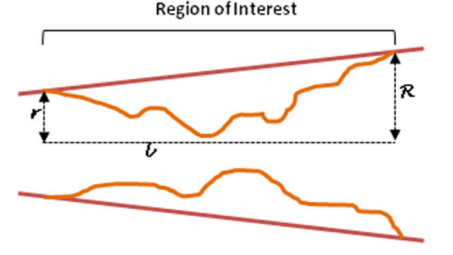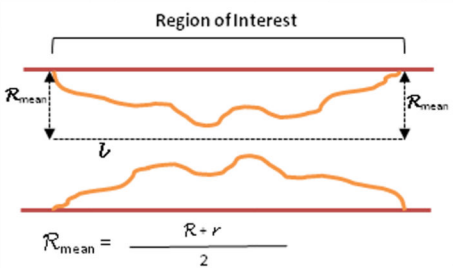
Figure 3. The three methods for pre-stenting (athero)-thrombotic volume measurement.
Intra- and interobserver reproducibility are reported for each strategy. (h= cross section thickness; l: region of interest length n= number of frames within region of interest; R= mean proximal reference radius; r: mean distal reference radius)
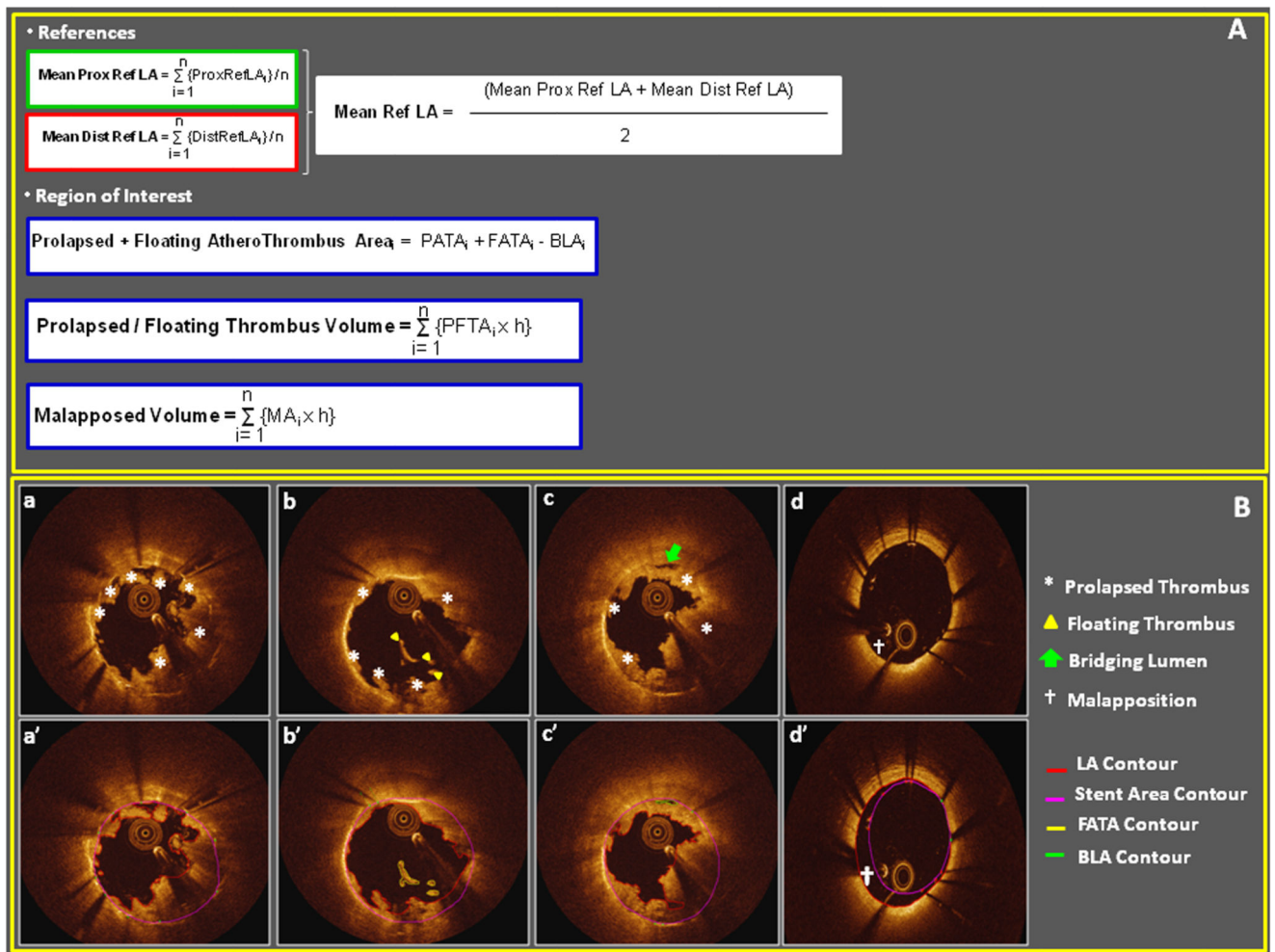
Figure 4. Post-stenting FD-OCT run measures.
Panel A. Mathematical formulas adopted to calculate prolapsed+floating atherothrombotic volume and malapposed volume. Panel B. Examples of prolapsed atherothrombotic material (asterisks in subpanel a, b and c and red contour in subpanel a'), floating atherothrombotic material (yellow arrowhead in subpanel b and yellow contour in subpanel b'), bridging lumen (green arrow in subpanel c and green contour in subpanel c') and malapposition († symbol in subpanel d and d').
(BLA: bridging lumen area; FATA: floating athero-thrombus area; LA: lumen contour; ref: reference; ROI: region of interest)

Figure 5. Relationship between post-stenting IMR, delta IMR and delta athero-thrombotic volume.
(ATV: delta athero-thrombus volume; IMR: index of microcirculatory resistance)

Table 1
Clinical and Procedural Characteristics.

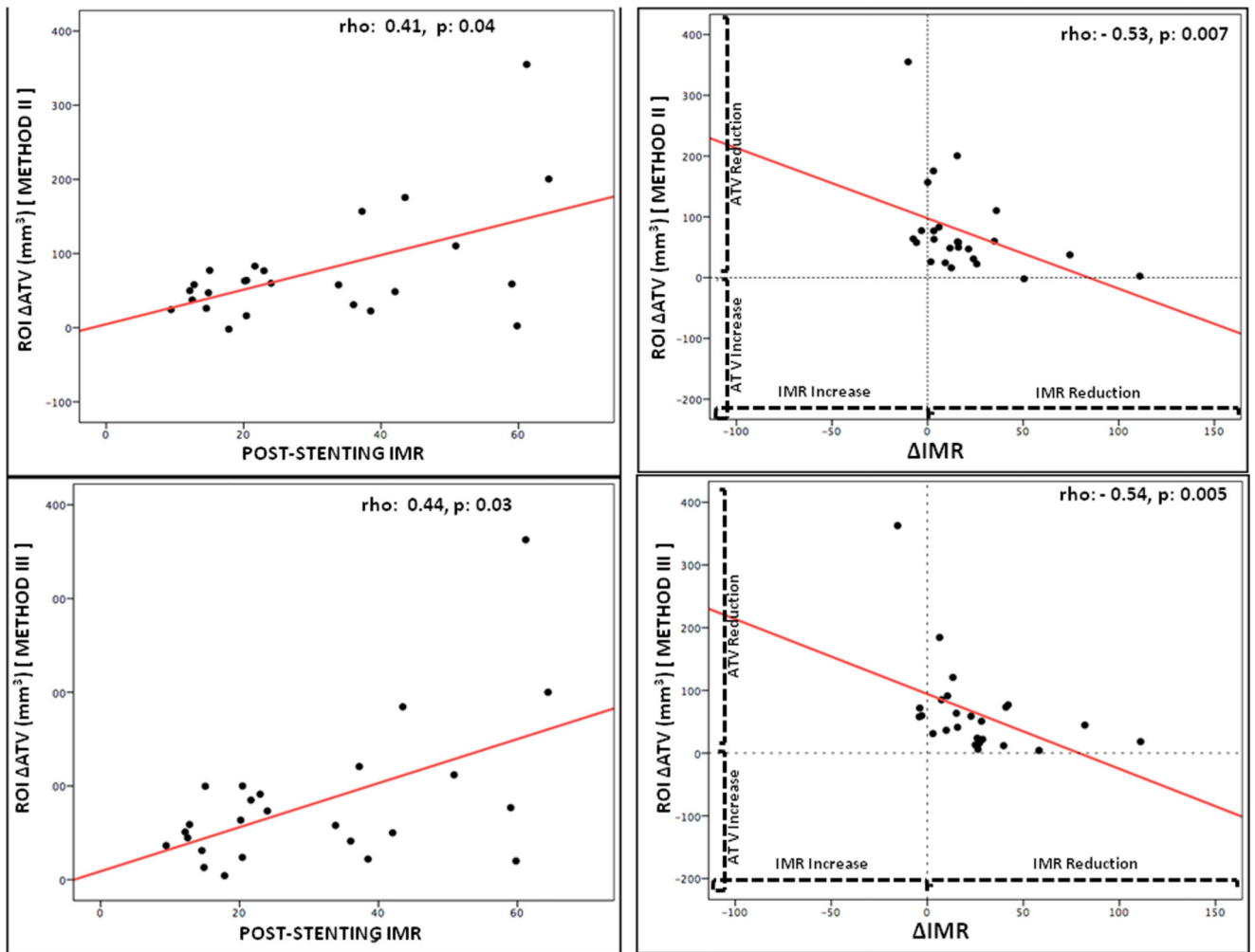Continuous normally-distributed variables are presented as mean ± standard deviation. Continuous not-normally-distributed variables are presented as median (interquartile range). Frequencies are expressed as number (percentage).

(BARI: Bypass Angioplasty Revascularization Investigation; DES: drug eluting stent; ECG: electrocardiographic; GPIIbIIIa: glycoprotein IIbIIIa; IHD: Ischemic Heart disease; IMR: index of microcirculatory resistance; LAD: left anterior descending; LCx: left circumflex; MBG: myocardial blush grade; MLD: minimal lumen diameter;RCA: right coronary artery; TIMI: thrombolysis in myocardial infarction; 2D QCA: two dimensional quantitative coronary angiography; %DS: percentage of diameter stenosis;   STR: ST resolution)

	Whole Cohort *(25 pts)*
Male gender	22 (88.8)
Age	58.2 ± 10.0
Hypertension	10 (40.0)
Hypercholesterolemia	9 (36.0)
Diabetes mellitus	2 (8.0)
Active Smoker	15 (60.0)
Family History of IHD	11(44.0)
Previous Cardiological History	9 (36.0)
Pain to wire time	
< 3 hours	12 (48.0)
3 hours and < 6 hours	9 (36.0)
6 hours	4 (16.0)
Culprit vessel	
LAD	10 (40.0)
LCx	1 (4.0)
RCA	14 (56.0)
TIMI flow at presentation	
0	20 (80.0)
1	2 (8.0)
2	2 (8.0)
3	1 (4.0)
Vessel closed at presentation	21 (84.0)
Thrombus Score	
0-1-2	4 (16.0)
3	5 (20.0)
4	16 (64.0)
5	0 (0.0)
Rentrop Score	

	Whole Cohort *(25 pts)*
0	20 (80.0)
1	3 (12.0)
2	2 (8.0)
3	0 (0.0)
Number vessel disease	
1	19 (76.0)
2	4 (16.0)
3	2 (8.0)
Syntax Score	7.0 (4.0- 9.5)
BARI Jeopardy Score	29.3 ± 7.7
Troponin peak (ng/ml)	110.4 (36.6 – 209.6)
Troponin AUC	185.3 (89.7 – 315.0)
Creatinin (μmol/ml)	74.4 ± 13.7
Periprocedural Medications	
Aspirin	25 (100.0)
Clopidogrel	25 (100.0)
Bivalirudin	25 (100.0)
GPIIbIIIa inhibitors	
Total adopted	5 (20.0)
Bail out	5 (20.0)
Thrombus Aspiration	23 (92.0)
Predilation	25 (100.0)
Max balloon diameter (mm)	2.5 ± 0.3
Present 2D-QCA	
MLD (mm)	1.31± 0.53
%DS	54.1 ± 15.2
Lesion Length (mm)	16.5 ± 8.5
DES	23 (92.0)
2nd generation	22 (88.0)
PES	1 (4.0)
EES	20 (80.0)
ZES	2 (8.0)
Number of stents	
1	23 (92.0)
2	2 (8.0)
3	0 (0.0)
Stent length (mm)	24.0 (18.0 - 32.0)
Stent Diameter (mm)	3.5 (3.0 – 4.0)
Postdilation	20 (80.0)

	Whole Cohort *(25 pts)*
Number of postdilations	2.0 (1.0 – 3.0)
Max postdilation pressure (atm)	16.3 ± 2.9
Max balloon diameter (mm)	3.8 ± 0.6
Final TIMI flow	
0	0 (0.0)
1	0 (0.0)
2	0 (0.0)
3	25 (100.0)
MBG	
0-1	2 (8.0)
2	9 (36.0)
3	14 (56.0)
Incomplete STR (< 70%)	4 (16.0)
Angiographic Distal Embolization	1 (4.0)
MBG < 2 and/or Incomplete STR (< 70%)	6 (24.0)

Table 2
Pre-stenting Optical Coherence Tomography Characteristics.

Continuous not-normally-distributed variables are presented as median (interquartile range). Frequencies are expressed as number (percentage).

(ATV: athero-thrombus volume; IMR: index of microcirculatory resistance; LA: Lumen Area; LD: lumen diameter; ROI: region of interest; TV: thrombus volume)

	Whole Cohort *(25 pts)*
PRE-STENTING	
REFERNCES	
Proximal Reference LA, mm²	8.34 (6.36 – 10.26)
Proximal Reference LD, mm	3.25 (2.83 – 3.61)
Distal Reference LA, mm²	6.87 (3.61 – 8.43)
Distal Reference LD, mm	2.95 (2.14 – 3.27)
Mean Reference LA, mm²	7.46 (5.23 – 9.67)
ROI	
Length, mm	23.2 (16.8 – 29.0)
Mean LA, mm²	4.86 (3.88 – 6.35)
Minimal LA, mm²	1.35 (1.03 – 1.88)
Mean LD, mm	2.39 (2.15 – 2.74)
Minimal LD, mm	1.31 (1.14 – 1.54)
Mean Thrombus Arch, •	120.0 (98.2 – 155.0)
Max Thrombus Arch, •	301.5 (218.1 – 347.7)
COCTAIL score	96.0 (80.5 – 179.5)
TV, mm³ (Method I)	14.65 (7.13 – 35.98)
ATV, mm³ (Method II)	67.59 (43.90 – 96.40)
ATV, mm³ (Method III)	68.01 (44.76 – 111.40)
POST-STENTING	
REFERENCES	
Proximal Reference LA, mm²	9.29 (7.12 – 11.28)
Proximal Reference LD, mm	3.43 (2.99 – 3.79)
Distal Reference LA, mm²	8.22 (5.26 – 9.94)
Distal Reference LD, mm	3.23 (2.58 – 3.55)
Mean Reference LA, mm²	8.66 (6.56 – 10.59)
STENTED SEGMENT	
Length, mm	23.2 (16.8 – 29.0)
Mean LA, mm²	9.45 (7.13 – 11.34)
Minimal LA, mm²	7.34 (5.35 – 8.71)
Mean LD, mm	3.47 (3.00 – 3.79)
Minimal LD, mm	3.06 (2.61 – 3.30)

	Whole Cohort *(25 pts)*
Mean SA, mm²	9.70 (7.59 – 12.10)
Minimal SA, mm²	8.20 (5.54 – 9.65)
Mean SD, mm	3.51 (3.10 – 3.92)
Minimal SD, mm	3.23(2.66 – 3.50)
%Covered Struts	52.42 (37.32 – 64.89)
%Uncovered Struts	42.07 (30.16 – 58.38)
%Malapposed Struts	2.90 (0.43 – 7.09)
Mean Prolapsed Athero-Thrombus Thickness, mm	0.05 (0.03 – 0.07)
Max Prolapsed Atero-Thrombus Thickness, mm	0.14 (0.09 – 0.20)
Mean Prolapsed +Floating Athero-Thrombus Area, mm²	0.48 (0.31 – 0.72)
Max Prolapsed +Floating Athero-Thrombus Area, mm²	1.50 (1.09 – 2.32)
Mean Prolapsed +Floating Athero-Thrombus Burden, %	5.46 (3.64 – 7.87)
Max Prolapsed +Floating Athero-Thrombus Burden, %	17.27 (11.23 – 23.25)
Prolapsed +Floating Athero-Thrombus Volume, mm³	10.79 (7.60 – 17.47)
Mean Malapposed Thickness, mm	0.00 (0.0- 0.01)
Max Malapposed Thickness, mm	0.03 (0.01 – 0.07)
Mean Malapposed Area, mm²	0.02 (0.01 – 0.10)
Max Malapposed Area, mm²	0.38 (0.14 – 0.93)
Mean Malapposed Burden, %	0.33 (0.05 – 0.86)
Max Malapposed Burden, %	1.15 (1.29 – 9.32)
Malapposed Volume, mm³	0.70 (0.13 – 2.97)
Intrastent Dissection	8 (32.0)
Intrastent Dissection Max Length, mm	0.50 (0.26 – 0.81)
Intrastent Dissection Mean Length, mm	0.78 (0.35 – 1.14)
Intrastent Dissection Longitudinal Extension, mm	0.07 (0.04 – 1.35)

Table 3

Relationship between variations of atherothrombotic volume and indices of coronary physiology.

Correlation are expresses by rho Spearman's coefficient. p< 0.05 is considered statistically significant. Cells containing statistical significant correlations are highlighted in red. (ATV: delta athero-thrombotic volume; CFR ; ATV: athero-thrombotic colume; CFR: coronary flow reserve; FFR: fractional flow reserve; IMR: index of microcirculatory resistance; PFATV: prolapsed+floating atherothrombotic volume; CFR ; delta CFR; FFR : delta FFR; IMR: delta IMR)

	ATV (ATV – PFATV) [Method II]	
	rho	p
FFR (FFR$_{pre\text{-}stenting}$ –FFR$_{post\text{-}stenting}$)	-0.22	0.28
CFR (CFR$_{pre\text{-}stenting}$ –CFR$_{post\text{-}stenting}$)	0.20	0.34
IMR (IMR$_{pre\text{-}stenting}$ –IMR$_{post\text{-}stenting}$)	-0.53	0.007
	ATV (ATV – PFATV) [Method III]	
	rho	p
FFR (FFR$_{pre\text{-}stenting}$ –FFR$_{post\text{-}stenting}$)	- 0.25	0.23
CFR (CFR$_{pre\text{-}stenting}$ –CFR$_{post\text{-}stenting}$)	- 0.14	0.50
IMR (IMR$_{pre\text{-}stenting}$ –IMR$_{post\text{-}stenting}$)	-0.54	0.005